

# Surface-Functionalized Nanoparticle Library Yields Probes for Apoptotic Cells

Eyk A. Schellenberger, Fred Reynolds, Ralph Weissleder,\* and Lee Josephson<sup>[a]</sup>

We have developed techniques for the efficient synthesis and screening of small libraries of surface-functionalized nanoparticles for the recognition of specific types of cells. To illustrate this concept we describe the development of a nanoparticle that preferentially recognizes apoptotic Jurkat cells in a manner similar to the apoptosis-recognizing protein annexin V. The nanoparticle, which is detectable by fluorescence or NMR relaxometry, was analyzed for

the ability to recognize normal and apoptotic cells by fluorescence-activated cell sorting (FACS) analysis and fluorescence microscopy. The capability to develop nanoparticles which interact with specific target cells could be applied to the design of materials for diverse applications including quantum dots, which serve as fluorescence tracers, colloidal gold, which serves as a tracer for electron micrographs, or the crystalline forms of drugs.

## Introduction

Techniques for the rapid synthesis and screening of compounds are fundamental to the rapid pace of progress in biological and pharmaceutical research. However, the application of these principles to the design of nanoparticle surfaces has not been achieved, primarily because of a lack of methods for rapidly modifying surfaces, chemically characterizing those modified surfaces, and testing the surfaces for biological activity. Such techniques could provide novel strategies for the development of a wide range of materials for medical applications whose surface imparts important functional properties. Surface-functionalized nanoparticle-sized materials (5–100 nm) have been made of gold,<sup>[1, 2]</sup> dextran-coated iron oxide,<sup>[3]</sup> quantum materials,<sup>[4, 5]</sup> or drug carriers.<sup>[6, 7]</sup>

Here we describe the parallel synthesis of surface-functionalized nanoparticles that are both magnetic and fluorescent and their interaction with normal and apoptotic cells. We chose nanoparticles because in addition to being amenable to surface modification they have a superparamagnetic core, which enables them to be used in applications such as MR imaging,<sup>[8, 9]</sup> cell separation,<sup>[10]</sup> or as magnetic sensors.<sup>[11]</sup> In addition the nanoparticles are fluorescent which allows interactions with cells to be quantified by fluorescence-activated cell sorting (FACS) analysis or fluorescence microscopy. As a model target we chose apoptotic cells, because the degree of apoptosis is a hallmark of a variety of diseases.<sup>[12, 13]</sup> We hypothesized that it should be feasible to develop small-molecule-functionalized, multivalent nanoparticle conjugates that have preferential binding to apoptotic cells similar to annexin V, a protein commonly used in the design of apoptotic cell-specific probes.<sup>[14]</sup>

## Results and Discussion

We first obtained a microlibrary of surface-modified nanoparticle probes by attaching a variety of low-molecular-weight functional groups to a caged magnetic nanoparticle termed amino-CLIO (aminated dextran caged iron oxide, see Figure 1).<sup>[11, 15, 16]</sup>

The amino-CLIO nanoparticle was first modified by the attachment of three fluoresceins per particle to permit quantitation of cell-associated nanoparticles regardless of the number or type of surface functional groups that are subsequently attached. Surface functional groups were then attached by using *N*-succinimidyl 3-(2-pyridyldithio)propionate (SPDP). The 2-pyridine disulfide nanoparticle was stable<sup>[17]</sup> and was prepared in sub-gram quantities sufficient for smaller-scale reactions with

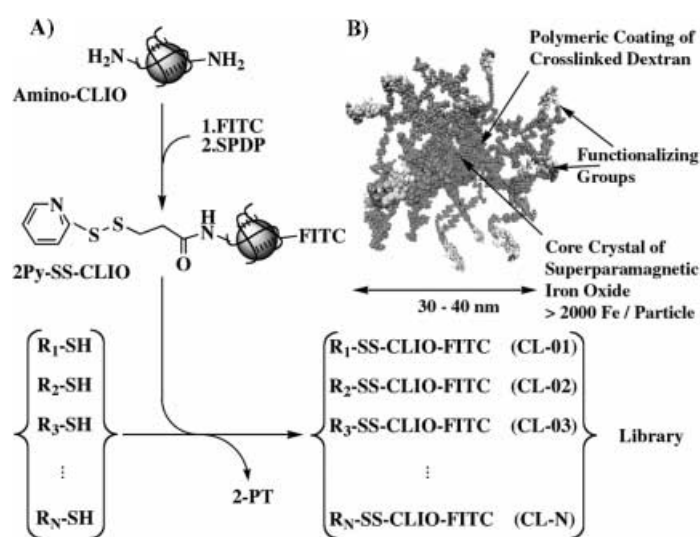


**Figure 1.** Parallel synthesis of surface-modified CLIO nanoparticles. A) The parent amino-CLIO nanoparticles were first labeled with FITC (2.7 per nanoparticle), then activated with SPDP, and reacted with thiol-containing surface modifiers ( $R-SH$ ). 2-PT release gives valency. B) Schematic model of a nanoparticle.

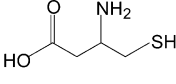
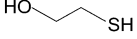
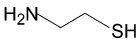
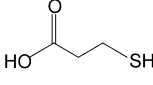
[a] Dr. E. A. Schellenberger, Dr. F. Reynolds, Prof. Dr. R. Weissleder, Prof. Dr. L. Josephson  
Harvard Medical School, Center for Molecular Imaging Research  
Building 149, 13th Street, 5403, Charlestown, MA 02129 (USA)  
Fax: (+1) 617-726-5708  
E-mail: weissleder@helix.mgh.harvard.edu

various R-SH surface-modifying compounds in a parallel fashion. The release of 2-pyridine thione (2-PT) after treatment with  $R_N$ -SH provided a method for determining the extent of surface modification and without direct examination of the surface.<sup>[18]</sup>

Representative examples from a larger array library produced (CL1–CL500) are summarized in Table 1 and were used for subsequent biological testing. The array consisted of negatively charged, positively charged, and neutral nanoparticles, of which initial screens showed that some positively charged nanoparticles bound apoptotic cells to a higher degree. Hence the behavior of selected positively charged and control nanoparticles is described here. Four low-molecular-weight thiol compounds (cysteine, 2-mercaptoethanol, mercaptoethylamine, and mercaptopropionic acid) were chosen as representative examples of two types of neutral surface groups (hydroxy and zwitterionic) and with surfaces consisting of negative or positive groups. Positively charged nanoparticles containing tripeptides (rGC-NH<sub>2</sub> and kGC-NH<sub>2</sub>) were also included. Finally, three representative peptides containing longer sequences of positively charged amino acids and C-terminal cysteine residues were included.

The ability of surface-functionalized nanoparticles from Table 1 to distinguish normal from apoptotic cells was first examined by FACS analysis, as shown in Figure 2, with results summarized in Figure 3. To determine how nanoparticles bind normal and apoptotic cells, cells were incubated with each of the fluorescein isothiocyanate (FITC)-labeled surface-functionalized CLIO nanoparticles together with Cy5.5-annexin V, and analyzed

**Table 1.** Representative surface-functionalized magnetic nanoparticles from a larger library tested (see Figure 1).

Nano-particle	$R_N$ -SH	$R_N$ /CLIO	Guanidinium	-NH <sub>2</sub>	-COOH
CL-42	rGC-SH	43	43	43	0
CL-45	rrrrGrrrrGC-SH	43	344	43	0
CL-35	kkkkGkkkkGC-SH	43	0	387	0
CL-11		43	0	43	43
CL-16		43	0	0	0
CL-30		43	0	43	0
CL-20		43	0	0	43
CL-32	kGC-SH	43	0	86	0
CT-62	GRKKRRQRRRGYKC-SH	9	45	27	0
CT-64	GRKKRRQRRRGYKC-SH	29	145	87	0

All peptides are C-terminal amides, which are not considered as primary amines. Peptide-SH groups used for attachment to CLIO are in italics.

by dual-wavelength FACS. Cy5.5 and FITC have sufficiently different optical properties that they can be used in dual-label FACS experiments without a need to correct for spillover. The top row of Figure 2 shows the results with the CL-45 nanoparticle. With untreated (Figure 2A) or camptothecin-treated cells

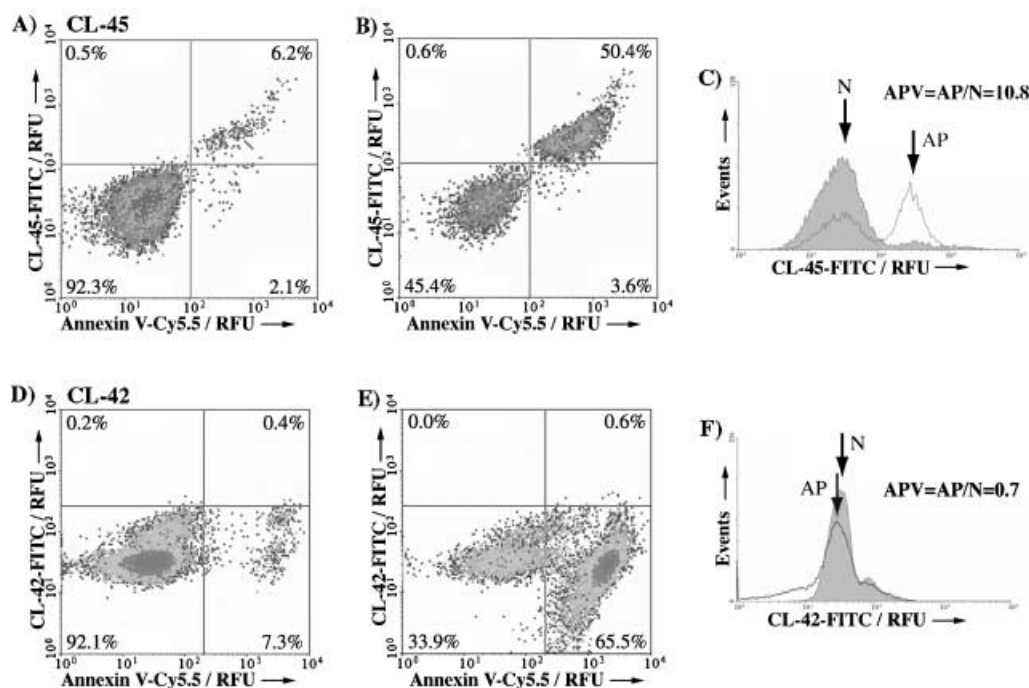


**Figure 2.** Screening of surface-functionalized nanoparticles for interaction with apoptotic cells. Dual-wavelength FACS analyses of A) untreated and B) treated cells incubated with Cy5.5-annexin V and CL-45 are shown (relative fluorescence units, RFU). Treatment results in apoptotic cells that bind both Cy5.5-annexin V and the nanoparticle. C) The distribution of FITC fluorescence for untreated cells (gray area) and camptothecin-treated cells (line). D) Data for untreated cells and E) treated cells incubated with Cy5.5-annexin V and CL-42. The median fluorescence of the predominant cell population before (gray area, N = normal) and after treatment (line, AP = apoptotic cells) are shown by arrows. An apoptotic preference value (APV = AP/N) was calculated from the medians as shown in (C) and F. Apoptotic preference values are presented in Figure 3.

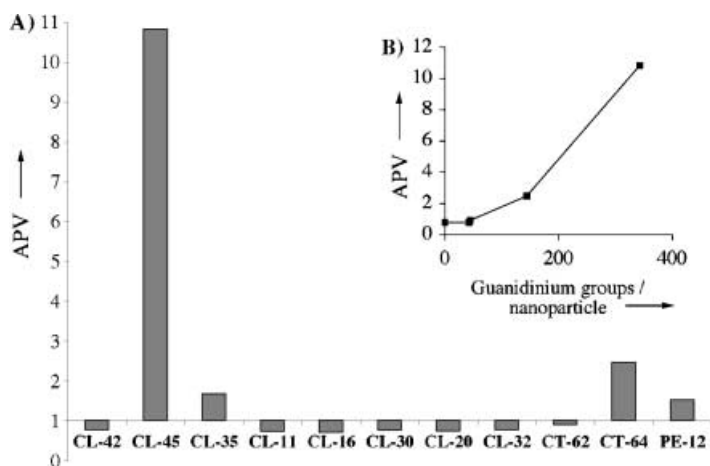


**Figure 3.** Apoptotic preference values (APVs) of compounds. A) The APV is the ratio of median fluorescence of apoptotic cells divided by the median fluorescence of normal cells. An APV greater than one indicates a preference for apoptotic cells, while less than one signifies a preference for normal cells. B) Relationship between the APV and the number of guanidinium groups per nanoparticle. The designation CL denotes a multivalent nanoparticle. PE-12 is the monovalent polyarginine peptide used to synthesize the CL-45.

(Figure 2B), cells bound both Cy5.5-annexin V and CL-45 in a virtually identical fashion more than 95% of the time. For treated cells, 45.4% bound no probe at all and 50.4% of cells bound both (total similar binding = 45.4% + 50.4% = 95.8%). For untreated cells the total amount of similar binding was 98.5% (i.e., 92.3% + 6.2%). To compare the preference of probes for apoptotic versus normal cells we divided the median of apoptotic cells by the median of normal cells (Figure 2). An apoptotic preference value (APV) of 10.8 was obtained for CL-45, which is significantly higher than for any of the other compounds. The preferential binding of CL-45 to apoptotic cells observed was confirmed by 1) demonstrating the ability of CL-45 to selectively remove apoptotic cells by magnetic cell fractionation and, 2) demonstrating that CL-45 was a better antagonist of the binding of FITC-annexin V to apoptotic cells than annexin V attached to the same nanoparticle by using a FACS displacement assay of FITC-annexin V<sup>[19, 20]</sup> (data not shown).

The opposite result, that is nanoparticles selective for normal cells, was obtained with the CL-42 nanoparticle as shown in Figures 2D–F. Unlike the preference for apoptotic cells shown by CL-45 (APV = 10.8), CL-42 had a preference for normal rather than apoptotic cells with an APV of 0.7. To assess whether the recognition of apoptotic cells with CL-45 was a result of the number of positive charges, we analyzed the behavior of CL-35, a nanoparticle in which primary amines replace guanidinium groups. CL-35 nanoparticle had only a slight preference for apoptotic cells with an APV of 1.7. Hence the selectivity for apoptotic cells was enhanced when the positive charge on the nanoparticle was provided by a guanidinium group rather than by a primary amine. Indeed, when cellular binding to apoptotic cells was plotted against the number of guanidinium groups attached, a nonlinear relationship was observed (Figure 3B, inset). Nanoparticles with a variety of neutral, negative, and positively charged surfaces acted similarly to CL-42 and had

APVs between 0.6 and 0.8 (Figure 3A). Furthermore, a monovalent fluorescein-labeled d-polyarginine control peptide with eight guanidinium groups (PE-12), but which was not conjugated to the CLIO nanoparticle, exhibited a low APV (Figure 3A).

We determined the cellular localization of CL-45 in apoptotic cells and compared it to that of annexin V. Figures 4A–C show five cells, two of which have membrane-localized CL-45 and Cy5.5-annexin V. As shown in Figure 2B for a sample of cells, cells labeled with CL-45 were labeled with Cy5.5-annexin V, and both probes were localized to the plasma membrane (Figure 4).

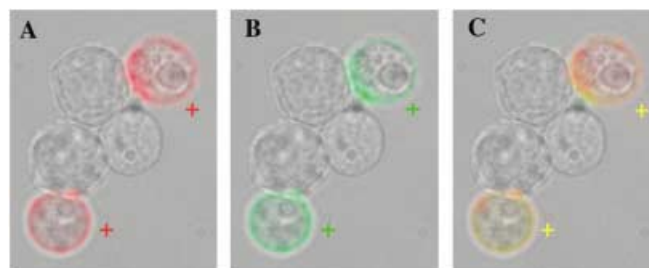


**Figure 4.** Dual-label fluorescence microscopy of camptothecin-treated Jurkat T cells (overlay with phase contrast image). Images of Cy5.5-annexin V, a reference label for apoptotic cells, and FITC-labeled CL-45 are shown in (A) and (B), respectively. Two cells out of five cells bind both, annexin V and CL-45 (C), while three cells are negative for both probes. These results confirm the high selectivity of CL-45 for apoptotic cells, as shown by FACS analysis (Figure 2).

We have employed a new approach to the design of cell-specific probes by using nanoparticles with small surface functional groups rather than by conjugating biological molecules such as antibodies or proteins. We term these materials “biomimetic nanoparticles”, since the selectivity for biological targets (apoptotic cells in this specific example but extendable to other cell populations) can be achieved through multivalent small molecules, which collectively mimic the function of larger proteins (annexin V in this example). In common with some phage display selection methods,<sup>[21, 22]</sup> our screening method utilizes cells in different functional states without knowledge of the molecular target. Unlike phage screening methods in which an amino acid sequence is deduced and synthetic peptides labeled to verify binding, we utilized a spatially encoded panel of magnetofluorescent nanoparticles. Screening is performed after labeling and surface functionalization, so that multivalent compounds can be screened.

Larger panels of surface-functionalized magnetic nanoparticles can be developed with the chemistry shown in Figure 1, since peptide- and oligonucleotide-functionalized nanoparticles exhibit excellent stability.<sup>[16]</sup> Key elements in the efficient synthesis and screening of surface modified nanoparticles are 1) the parallel synthesis of using a single batch of fluorescent, SPDP-activated nanoparticles, followed by reaction with a panel of thiol compounds (see Figure 1); 2) the extent of surface modification is determined indirectly, from the 2-PT release rather than for direct surface analysis; 3) the fluorochrome attached directly to the nanoparticle allows the screening by FACS, as performed here, or by a wide range of high-throughput fluorescence-based screening methods; 4) the separation of

small, surface-functionalizing groups (< 5 kDa) from the magnetic nanoparticles ( $\approx 1000$  kDa) by batchwise separators designed for oligonucleotide labeling, leading to libraries of thousands of compounds; and 5) the ability to attach different types of molecules to nanoparticles including peptides, oligonucleotides, proteins, and low-molecular-weight molecules by using the chemistry described here.<sup>[3, 11, 15, 16]</sup>

## Conclusion

The rapid parallel synthesis of labeled nanoparticles outlined may open the way for the design of a wide range of biomimetic nanoparticle probes, generating selectivity for a wide range of specific cells (e.g., T cell subsets, activated macrophages, NK cells) through multivalent surface modification. The combination of magnetic and fluorescent properties provided may permit use of our nanoparticles as MR-imaging probes, for cell sorting, and for an improved understanding of the interactions between the surfaces of cells and materials.

## Experimental Section

**Preparation of surface-functionalized nanoparticles:** Peptides were synthesized by using Fmoc chemistry on Rink amide resin (Calbiochem, NovaBiochem) and were purified by reversed-phase HPLC. The peptide molecular weights obtained were analyzed by mass spectrometry (MALDI-TOF). Peptides were within 1 Da of their calculated values. Peptides were kGC-NH<sub>2</sub> (d-lys), rGC-NH<sub>2</sub>, kkkkGkkkGC-NH<sub>2</sub>, rrrrGrrrGC-NH<sub>2</sub>, or the corresponding fluoresceinated peptide, rrrrGrrrGK(FITC)-NH<sub>2</sub>, and GRKKRRRRRGYKC-NH<sub>2</sub>. All peptides had C-terminal amide residues. Mercaptoethanol, mercaptoethylamine, and mercaptopropionic acid were from Sigma Chemical.

The amino-CLIO nanoparticle was synthesized by crosslinking the dextran-coated nanoparticle with epichlorohydrin and reaction with ammonia to provide primary amine groups.<sup>[15, 16]</sup> 9 mL of amino-CLIO (100 mg Fe in 8.6 mL sodium citrate, pH 8.0) was added to phosphate-buffered saline (PBS; 8 mL, pH 7.4). Fluorescein isothiocyanate (FITC, Molecular Biosciences; 20 mM in 300  $\mu$ L DMSO) was added and the reaction was incubated for 2 h at room temperature. The FITC-labeled nanoparticle was separated from unreacted FITC by gel filtration (Sephadex G25, 0.02 M sodium citrate, pH 8.2). Iron was determined spectrophotometrically and the nanoparticle number was calculated by assuming 2064 Fe atoms per nanoparticle.<sup>[23]</sup> *N*-Succinimidyl 3-(2-pyridylthio)propionate (SPDP, Molecular Biosciences, 60 mM in 3.6 mL DMSO) was added and the mixture was incubated for 2 h at room temperature. Low-molecular-weight impurities were removed by dialysis against an aqueous solution of sodium citrate (0.02 M; pH 8.3) and sodium chloride (0.15 M). We determined the number of FITC fluorochromes per nanoparticle spectrophotometrically ( $E_{494} = 73\,000\text{ M}^{-1}\text{ cm}^{-1}$ ), after subtracting the background absorbance from amino-CLIO. We determined the number of 2-pyridine disulfide groups per nanoparticle by the release of pyridine-2-thione (2-PT) spectrophotometrically ( $E_{343} = 8100\text{ M}^{-1}\text{ cm}^{-1}$ ).<sup>[18]</sup> The resulting preparation of 2-pyridine disulfide, FITC-modified CLIO nanoparticles had an average of three fluorescein residues and 43 2-pyridine disulfides per nanoparticle. The nanoparticles were 35 nm in size as measured by photocorrelation spectroscopy (Zetasizer 1000 SHA, Malvern Instruments), and R1 and

R2 relaxivities of 20.8 and 41.5  $\text{mm}^{-1}\text{ s}^{-1}$  (0.47-T Bruker MR spectrometer).

To prepare surface-modified nanoparticles, thiol compounds (R-SH in Figure 1 and see Table 1; 100  $\mu$ L, 50 mM) were prepared in PBS (pH 8.0) and were added to 2-pyridine disulfide-CLIO nanoparticles (0.5 mL, 3.5 mg  $\text{Fe mL}^{-1}$ ). The reaction was incubated for 2 h at room temperature. Unreacted surface-modifying thiols were separated from nanoparticles by gel filtration (Sephadex G25, 0.02 M sodium citrate, 0.15 M NaCl, pH 8.3).

**Preparation of Cy5.5-annexin V:** Annexin V (Theseus Imaging Corp.) was reacted with the *N*-hydroxysuccinimide ester of the Cy5.5 (Amersham-Pharmacia) as described.<sup>[19, 24]</sup> The conjugate had 1.1 Cy5.5 dyes attached per mole of protein.

**Cell culture:** Jurkat T cells (Clone E6-1, ATCC number TIB-152) were grown in RPMI 1640 medium in 10% fetal bovine serum (Vitacell number 30-2021, ATCC) changed every 2 or 3 days. Apoptosis was induced by the addition of 7  $\mu$ L camptothecin (1 mM in DMSO) per mL culture medium for 5-6 h. Induction of apoptosis was verified by staining with propidium iodide and FITC-Annexin V (Clontech) in calcium-containing binding buffer (BB; 1.8 mM CaCl<sub>2</sub>, 10 mM HEPES, 150 mM NaCl, 5 mM KCl, 1 mM MgCl<sub>2</sub>, pH 7.4). The cells were analyzed with a FACS-Calibur cytometer (Becton Dickinson) according the manufacturer's manual (FL1 fluorescence channel FITC-annexin V and FITC-CLIO nanoparticle; FL4 fluorescence channel for Cy5.5-annexin V).

**Binding of surface-modified nanoparticles to Jurkat T cells:** After induction of apoptosis (as above) about  $6 \times 10^4$  cells were washed twice and then resuspended in 200  $\mu$ L BB. Cells were then incubated with 3.6 pmol of the CLIO derivatives (2.8  $\mu$ g  $\text{Fe mL}^{-1}$  or 25 nm CLIO particles final concentration) for 10 min at room temperature. In addition, cells were incubated with 0.1  $\mu$ g Cy5.5-annexin V for the double label experiments. After adding 500  $\mu$ L BB, FACS analysis was performed (as above, FL1 and FL4 fluorescence channel).

**Fluorescence microscopy:** After incubation with CL-45 and Cy5.5-annexin V as above, 10  $\mu$ L of the cell suspension was applied to the slide, placed on an Axiovert Zeiss microscope (Carl Zeiss Micro-Imaging), and photographed by employing an SenSys CCD-camera (Roper Scientific) attached to a G4-PowerMac (Apple Computer). Images of light, FITC, and NIRF channel were acquired.

## Acknowledgements

The authors would like to acknowledge the help of Terence O'Loughlin in modeling the CLIO structure. Work was supported in part by NIH grants RO1CA86782, P50CA86355, R24CA92782, R01EB000662, and CA91807. E.A.S. was supported in part by a grant from the "Deutsche Akademie der Naturforscher und Mediziner Leopoldina" and the CMIR Development Fund.

**Keywords:** apoptosis • fluorescence • nanostructures • peptides • screening • surface chemistry

- [1] R. Elghanian, J. J. Storhoff, R. C. Mucic, R. L. Letsinger, C. A. Mirkin, *Science* **1997**, 277, 1078.
- [2] J. M. Robinson, T. Takizawa, D. D. Vandre, R. W. Burry, *Microsc. Res. Tech.* **1998**, 42, 13.
- [3] J. M. Perez, T. O'Loughlin, F. J. Simeone, R. Weissleder, L. Josephson, *J. Am. Chem. Soc.* **2002**, 124, 2856.
- [4] M. Han, X. Gao, J. Z. Su, S. Nie, *Nat. Biotechnol.* **2001**, 19, 631.

- [5] W. C. Chan, S. Nie, *Science* **1998**, *281*, 2016.
- [6] J. D. Hood, M. Bednarski, R. Frausto, S. Guccione, R. A. Reisfeld, R. Xiang, D. A. Cheres, *Science* **2002**, *296*, 2404.
- [7] D. D. Spragg, D. R. Alford, R. Greferath, C. E. Larsen, K. D. Lee, G. C. Gurtner, M. I. Cybulsky, P. F. Tosi, C. Nicolau, M. A. Gimbrone, Jr., *Proc. Natl. Acad. Sci. USA* **1997**, *94*, 8795.
- [8] R. Weissleder, A. Moore, U. Mahmood, R. Borade, H. Benveniste, E. A. Chiocca, J. P. Babilion, *Nat. Med.* **2000**, *6*, 351.
- [9] M. G. Harisinghani, J. Barentsz, P. F. Hahn, W. M. Deserno, S. Tabatabaei, C. H. van de Kaa, J. de la Rosette, R. Weissleder, *N. Engl. J. Med.* **2003**, *348*, 2491.
- [10] A. G. Tibbe, B. G. de Grooth, J. Greve, P. A. Liberti, G. J. Dolan, L. W. Terstappen, *Nat. Biotechnol.* **1999**, *17*, 1210.
- [11] J. M. Perez, L. Josephson, T. O'Loughlin, D. Hogemann, R. Weissleder, *Nat. Biotechnol.* **2002**, *20*, 816.
- [12] J. F. Kerr, A. H. Wyllie, A. R. Currie, *Br. J. Cancer* **1972**, *26*, 239.
- [13] C. B. Thompson, *Science* **1995**, *267*, 1456.
- [14] S. J. Martin, C. P. Reutelingsperger, A. J. McGahon, J. A. Rader, R. C. van Schie, D. M. LaFace, D. R. Green, *J. Exp. Med.* **1995**, *182*, 1545.
- [15] L. Josephson, C. H. Tung, A. Moore, R. Weissleder, *Bioconjug. Chem.* **1999**, *10*, 186.
- [16] L. Josephson, J. M. Perez, R. Weissleder, *Angew. Chem.* **2001**, *113*, 3304; *Angew. Chem. Int. Ed.* **2001**, *40*, 3204.
- [17] J. Carlsson, H. Drevin, R. Axen, *Biochem. J.* **1978**, *173*, 723.
- [18] M. Zhao, M. F. Kircher, L. Josephson, R. Weissleder, *Bioconjug. Chem.* **2002**, *13*, 840.
- [19] E. Schellenberger, A. J. Bogdanov, A. Petrovsky, V. Ntziachristos, R. Weissleder, L. Josephson, *Neoplasia* **2003**, *5*, 187.
- [20] E. A. Schellenberger, A. J. Bogdanov, D. Hogemann, J. Tait, R. Weissleder, L. Josephson, *Mol. Imaging* **2002**, *1*.
- [21] M. Trepel, W. Arap, R. Pasqualini, *Curr. Opin. Chem. Biol.* **2002**, *6*, 399.
- [22] R. Pasqualini, W. Arap, D. M. McDonald, *Trends Mol. Med.* **2002**, *8*, 563.
- [23] T. Shen, R. Weissleder, M. Papisov, A. Bogdanov, Jr., T. J. Brady, *Magn. Reson. Med.* **1993**, *29*, 599.
- [24] A. Petrovsky, E. Schellenberger, L. Josephson, R. Weissleder, A. J. Bogdanov, *Cancer Res.* **2003**, *63*, 1936.

---

Received: July 11, 2003 [F 713]